International Journal of Botany Studies
ISSN: 2455-541X; Impact Factor: RJIF 5.12
Received: 09-10-2020; Accepted: 24-10-2020: Published: 12-11-2020
www.botanyjournals.com
Volume 5; Issue 6; 2020; Page No. 161-166

Synthesis and characterization of zinc oxide nanoparticles using *Vitex altissima* (L.) leaves extract and its Biological applications

Bhavana S[1], Vinod Gubbiveeranna[2], Kusuma CG[3], Sumachirayu CK[4], Ravikumar H[5], Nagaraju S[6*]
[1-4, 6] Department of Studies and Research in Biochemistry, Tumkur University, Tumakuru, India
[5] Department of Life Science, Jnana Bharthi Campus, Bangalore University, Bangalore, India

Abstract
Green synthesis of Zinc Oxide Nanoparticles (ZnO NPs) has gained a greater interest as a simple, cost effective and ecofriendly. In this study, the ZnO NPs were synthesized using *Vitex altissima* leaves extract by the combustion method. ZnO NPs were characterized by Powder X-Ray Diffraction (PXRD), UV-Visible spectroscopy, Fourier Transform-Infrared (FTIR) spectroscopy, Scanning Electron Microscope (SEM) and Transmission Electron Microscopy (TEM) techniques. The PXRD pattern of ZnO NPs showed hexagonal wurtzite structure with average crystalline sizes of 10-50 nm. The formation of ZnO NPs was confirmed by its maximum absorbance at 373 nm in UV-Visible spectroscopy. FTIR data showed the presence of different functional groups. Morphological studies were revealed by SEM and TEM. ZnO NPs showed an effective zone of inhibition in agar well diffusion assay for pathogenic gram positive (*Staphylococcus aureus*) and gram negative (*Escherichia coli* and *Pseudomonas desmolyticum*) bacteria confirming efficient antibacterial activity. ZnO NPs revealed an efficient antioxidant, anticoagulant and antiplatelet activity.

Keywords: antimicrobial, antioxidant, anticoagulant, antiplatelet, *Vitex altissima*, ZNO NPS

1. Introduction
In recent years, metal oxide Nanoparticles (NPs) have been utilized for biological applications such as drug/ gene delivery, bio-detection of pathogens, tissue engineering, diagnostics, cancer therapy due to their unique physicochemical and biological properties [1-2]. Because of its exclusive features like size, morphology and biocompatibility, it is exposed for biological applications. Zinc oxide is considered as an important material among transition metal oxide nanomaterials. ZnO has a high excitation binding energy of 60 MeV and wide semiconductor band gap of 3.37 eV. It is one of the binary compound in II to VI group of elements [3-8].
Several methods have been employed to synthesize ZnO nanoparticles such as sol–gel, direct precipitation, solvothermal and hydrothermal [9–13]. These methods require tedious procedures, expensive substrate and sophisticated equipment. In this study, Solution Combustion Synthesis (SCS) method was employed as it is a simple, easier, less energy and less time-consuming method among the existing wet chemical routes. Important benefits of green synthesis are lesser or zero pollution to the environment and nanomaterials can be synthesized easily, environmentally friendly and reasonable scale [14-16].
In the present work, the ZnO NPs were synthesized using aqueous extract of *Vitex altissima* leaves by solution combustion method. *V. altissima* is a woody plant belongs to a family verbenaceae and is widely spread in the Asian region and used as conventional medicines for various diseases such as allergies, urinary infection diseases, wounds, ulcers, inflammation and eczema [17-18]. The synthesized ZnO NPs were characterized by analytical techniques such as Powder X-Ray Diffraction (PXRD), UV-Visible spectroscopy, Fourier Transform-Infrared (FTIR) spectroscopy, Scanning Electron Microscope (SEM) and Transmission Electron Microscopy (TEM). Further, the biocompatible synthesized ZnO NPs were studied by different biological activities such as antimicrobial, antioxidant, anticoagulant, platelet aggregation and hemolytic activity.

2. Materials and methods
2.1. Materials
Vitex altissima [L.] plant leaves were collected from the Devarayanadurga forest area, Tumkur Dist., Karnataka, India. The plant was authenticated by Dr. Lakshmana, Department of Botany, Tumkur University, Tumkur. All the chemicals and reagents were used with Analytical Reagent grade (AR) without further purification. All the chemicals and reagents were purchased from Hi-Media Pvt. Ltd. Bangalore.

2.2. Preparation of extract and synthesis of ZnO Nanoparticles from *Vitex altissima*
Preparation of aqueous extract using *V. altissima* leaves was done by the soxhlet extraction apparatus [19]. ZnO Nanoparticles were synthesized by using aqueous extract of *V. altissima* leaves by solution combustion method [20]. In the present study, synthesis of ZnO NPs, was carried out by 1:1 ratio of Zinc nitrate hexahydrate (Zn (NO3)2.6H2O) as oxidizing agent and *V. altissima* leaves extracts as reducing agent were taken in a Petri dish, followed by adding a small amount of doubled distilled water and stirred at room temperature for 10-15 min with the help of magnetic stirrer at 1000 rpm to get a homogeneous solution. Ultimately, the above solution was introduced into the preheated muffle furnace at 400±10°C to initiate the reaction, the reaction was completed within 5±1 min and the product was produced in the form of powder and then the obtained product was further calcinated at 600°C for 3h to eliminate

the impurities. As a result, pure product is obtained and it is subjected to characterization and used to analyze different biological activities.

2.3. Characterization
Green synthesized ZnO NPs were characterized by X-ray diffraction studies with the help of Powder X-ray Diffractometer (PXRD-Shimadzu-7000) with monochromatized Cu Kα radiation. UV-Vis absorption studies of ZnO NPs were recorded using the Perkin Elmer Lamda-35 spectrophotometer. The IR study of ZnO NPs was analyzed with the help of the Perkin Elmer Spectrum BX FT-IR system. Morphological studies of ZnO NPs was analyzed by Scanning Electron Microscopy (Hitachi: Table Top Microscope Model TM 3000) and Transmission Electron Microscopy (TECNAIF-30) techniques.

2.4. Antibacterial activity
The antibacterial activity of ZnO NPs against bacterial pathogens both gram-positive (*Staphylococcus aureus*) and gram-negative (*Escherichia coli*, and *Pseudomonas desmolyticum*) strains is carried out in an aseptic condition [21]. Nutrient agar (NA) plates were prepared by Nutrient agar media (3.7% w/v). NA is dissolved in 100 mL of doubled distilled water and then autoclaved for 15 min. The autoclaved NA medium was transferred into sterilized petri-dishes and then left to solidify for some time. After solidifying the NA medium, inoculate 100 µL of 24 hrs mature specific bacterial cultural strains by spreading on the surface of the NA plates with the aid of an L-Shaped sterilized glass rod, then the wells of about 6 mm are made with the help of a steel cork borer in NA plates. Biosynthesized ZnO NPs were well dispersed in sterilized distilled water by using sonicator and then different concentrations of ZnO NPs (50, 100 and 150 µg/µL) using micro-pipettes are added to the well. At the same time, the standard bacterial drug ciprofloxacin as a positive control tested against the bacteria and then incubated for 24-36 hrs at 37°C. After incubation, the zone of inhibition of each well was observed and then measured in millimeter (mm). The experiment was performed in triplicates and then measured the average values and determined the antibacterial activity.

2.5. Antioxidant activity
Antioxidant activity of ZnO NPs was performed according to Brand-Williams method [22]. In this method different concentrations of ZnO NPs were allowed to react with DPPH (1 mM) solution and then incubated in a dark condition for 30 min at room temperature. After incubation the absorbance was recorded at 520 nm against the blank and also determined the IC_{50} value.

2.6. Anticoagulant, Platelet aggregation, and direct hemolytic activity
2.6.1. Human blood
During the experiment, fresh human blood was obtained from healthy donors.

2.6.2. Plasma re-calcification time
Plasma recalcification time was calculated by the method as follows [23]. The blood drawn from healthy volunteers are transferred to a tube containing 3.2% of sodium citrate (9:1). The tube is tilted slowly twice to mix blood with anticoagulant. Then this was subjected to centrifugation for 6 min at 3000 rpm to obtain platelet poor plasma. The different concentrations of ZnO NPs were pre-incubated with citrated human plasma for 5 min at 37°C. Then 25mM of calcium chloride ($CaCl_2$) was added to the pre-incubated mixture and the time for clotting was recorded.

2.6.3. Platelet aggregation
The turbid metric method [24] has been described by a dual-channel chronology. The human blood was drawn from healthy volunteers and centrifuged by adding 3.2% sodium citrate (9:1) for 10 min at 900 rpm to get platelet rich plasma (PRP). 0.25 ml of PRP was transferred to a glass cuvette containing a metal stirrer with Teflon coated. The aliquots of PRP were pre-incubated at 37^0C by constant stirring at 1200 rpm. The aggregation was initiated by adding ZnO NPs and ADP as agonist, the experiment was continued for 6 min. The trace of aggregation of nanoparticles has been noted and recorded.

2.6.4. Hemolytic activity
In vitro hemolytic activity was tested by the method [25]. The blood was centrifuged at 1500 rpm for five minutes to obtain 2 ml of tightly packed RBC. 2% erythrocyte suspension was prepared in sterile normal buffer saline. Different concentrations of ZnO Nps (0-350µg) were mixed with 0.5mL of a 2% erythrocyte suspension and 0.5 mL of normal saline. The solution was incubated for 30 min at 37^0C. After incubation, the reaction mixture volume was made up to 2ml with normal saline which was then centrifuged for 2-3 min at 1500 rpm. The amount of free hemoglobin in 1.0 mL of the supernatant was measured at 540nm. Normal saline and distilled water were used as minimal and maximal hemolytic controls.

3. Results and Discussions
Generally, the plant extracts possess different bioactive constituents. The aqueous extract of *Vitex altissima* leaves exhibiting the numerous bioactive secondary metabolites such as alkaloids, glycosides, triterpenoids, saponins and quinones. Herein, we have synthesized ZnO NPs using *V. altissima* leaves extract by solution combustion method which is simple, cost-effective, non-toxic, eco-friendly, and biocompatible. The structural, optical, and morphological studies of ZnO NPs were characterized by different analytical techniques such as PXRD, UV-Visible, FTIR, SEM and TEM. Further, the synthesized ZnO NPs were used to analyze various biological properties such as antimicrobial, antioxidant, anticoagulant, platelet aggregation, and hemolytic activity.

3.1. PXRD
The study of the phase and purity of the Nano crystallized ZnO NPs using aqueous extract of *V. altissima* leaves was analyzed by the PXRD pattern as shown in Fig.1. The diffraction pattern of the ZnO NPs are well-indexed to the hexagonal phase with a wurtzite structure with lattice parameter constants a, b = 3.25049 Å, c = 5.20263 Å which are firm with the values compare to standard data card JCPDS no.36-1451. By the PXRD pattern of ZnO NPs estimated the average particle size using Debye–Scherrer's formula [26].

$$D=\frac{K\lambda}{\beta cos\theta} \ldots\ldots\ldots\ldots\ldots\ldots \quad (1)$$

Where 'k' is shape factor (0.9), 'λ' is the wavelength of X-ray (1.5406 A °) Cu Kα radiation, 'β' is the full width at half maximum (FWHM), 'θ' is the Bragg angle, and 'D' is crystallite size. The average crystallite size of ZnO NPs was found to be 10-50 nm.

3.2. UV-Visible

UV-Visible analysis of synthesized ZnO NPs using aqueous extract of *Vitex altissima* leaves is shown in Fig.2. The UV-Visible absorption spectrum of ZnO NPs exhibited a typical excitation absorption band that appeared at 373 nm confirms the ZnO. The ZnO NPs absorption spectrum shows the sharp and prominent peak due to the shift of their electrons from the valence band to the conduction band. The band gap energy was estimated by the Tauc's relation [27].

$$\alpha h\upsilon = A\,(h\upsilon - E_g)^n \ldots\ldots\ldots\ldots\ldots \quad (2)$$

Where, 'h' is Planck's constant, 'v' is photon's frequency, 'α' is the absorption coefficient, E_g is the band gap and 'A' is proportionality constant.

3.3. FTIR

The FTIR analysis of synthesized ZnO NPs was performed to determine the functional groups recorded between in the range of 4000–500 cm^{-1} as shown in Fig.3. The broad prominent characteristic band at 3400 cm^{-1} is related to -OH stretching vibrations. The band of 2340 cm^{-1} belongs to Ar-H stretching vibration. The band of 1384 and 1045cm^{-1} is C-H and C-O and stretching vibrations [28,29]. The 1023 and 1150 cm^{-1} shows an absorption region consisting of C-O and C–N stretching vibrations. In addition to this, the band at 760 and 713 cm^{-1} is a C-H stretching vibrational mode of action. The peak in the range of 430–500 cm^{-1} is due to the presence of Zn–O bond. Some unresolved peaks in pattern may be due to some impurities.

3.4. Morphological analysis

The Morphological analyses of synthesized ZnO NPs are represented in Fig.4. SEM micrograph of ZnO NPs showed the particles are agglomerated and well-defined conical and triangular in shapes as shown in Fig. 4(a). The TEM micrograph of ZnO NPs exhibit the hexagonal structure and then found to be 50 nm in size as shown in Fig. 4 (b).

3.5. Antibacterial activity

The significant antibacterial activity of ZnO nanoparticles was tested against pathogenic bacterial strains *Staphylococcus aureus, Escherichia coli*, and *Pseudomonas desmolyticum* using the agar well diffusion method. The inhibition zone has been observed with different concentrations (50, 100 and 150 µg/mL) of ZnO NPs for individual strains respectively. The significant inhibition zone has been shown by *S. aureus* compared to *E. coli* and *P. desmolyticum* as shown in Fig.5 and Table.1. ZnO NPs interacting with the cell membrane of the bacteria and then allow ZnO particles to enter the cell and it may cause cell enzyme dysfunction and disruptions of the cell membrane by ZnO nanoparticles [30, 31, 32, 33].

3.6. Antioxidant activity

Antioxidants are bioactive compounds that serve as a scavenger of the Reactive Oxygen Species (ROS) by bringing an end to the oxidizing chain reaction. ROS plays a crucial role in the pathogenesis of a variety of degenerative disorders, including coronary and carcinogenic diseases. Typically, the DPPH assay is used to test the nanoparticle's radical scavenging capacity. The ZnO NPs significantly scavenged the DPPH radicles with an IC_{50} value of 3506 µg/mL as shown in Fig. 6 [34].

3.7 Plasma Recalcification time

At the site of injury, hemostasis is the physical phenomenon that prevents and stops bleeding. Therefore, ZnO NPs have been examined on the study of blood coagulation. Plasma recalcification time of ZnO NPs was determined by citrated human plasma and showed an increased clotting time as shown in Fig.7. Remarkably, different concentrations of ZnO NPs such as 120, 160, 200, 240, 280 µg with clotting time were 221, 269, 369, 420, and 467 seconds respectively and contrary to control $CaCl_2$ showed a clotting time of 177 Sec, indicates that ZnO NPs acts as an anti-coagulant [35, 36].

3.8. Platelet Aggregation study

Platelets are the significant modules in the way of the blood stream, their vital role in blood clotting has taken place at the site of injury by forming the platelet plug. In the physiological system, the different agonists such as ADP, collagen, thrombin, and coagulation factors binding upon with their respective receptors on the platelet membrane that leads to the aggregation process. Therefore, the ZnO NPs was studied for its effect on ADP induced platelet aggregation as shown in Fig.8 (a). The inhibition was found to be dose-dependent. The effect of platelet aggregation (%) of ZnO NPs (300µg/mL) is 54% as shown in Fig.8 (b). The Fig.8 (c) shows the inhibition (%) of ZnO NPs (300µg/mL) is 46%. Thus, the synthesized ZnO NPs could be an effective antiplatelet agent to treat health disorders such as thrombosis [37, 38].

3.9. Hemolytic activity

By identifying the role of ZnO NPs on the membrane of red blood cells, indicates that ZnO NPs did not hydrolyze the RBCs [39].

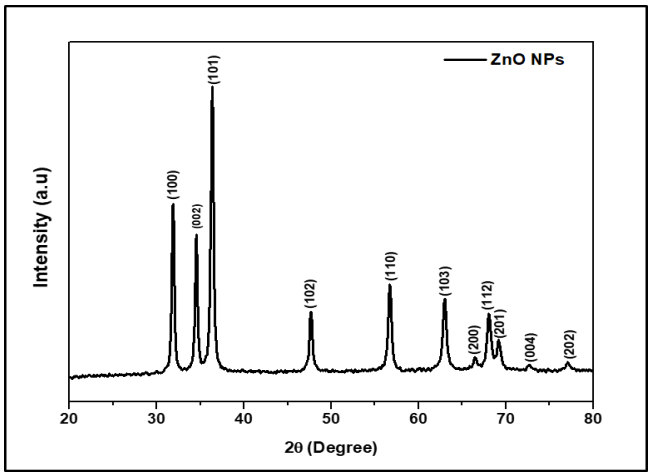

Fig 1: PXRD pattern of ZnO NPs from aqueous leaves extract of Vitex altissima

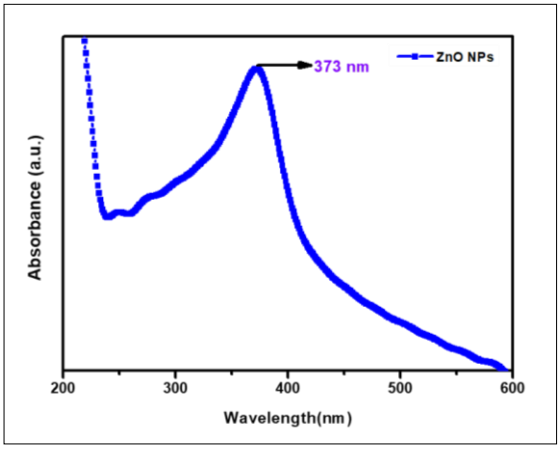

Fig 2: UV-Visible absorption spectrum of ZnO NPs from aqueous leaves extract of *Vitex altissima*

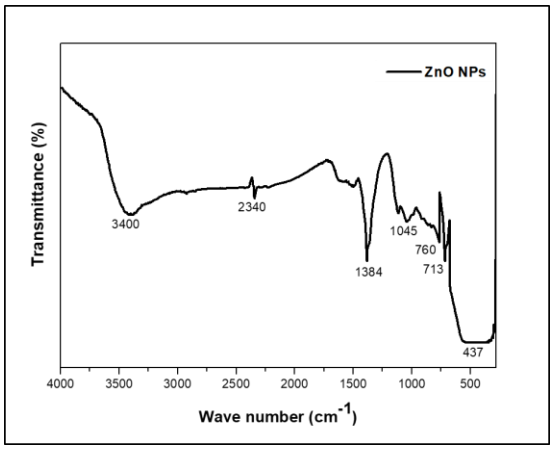

Fig 3: FT-IR spectrum of synthesis of ZnO NPs from aqueous leaves extract of *Vitex altissima*

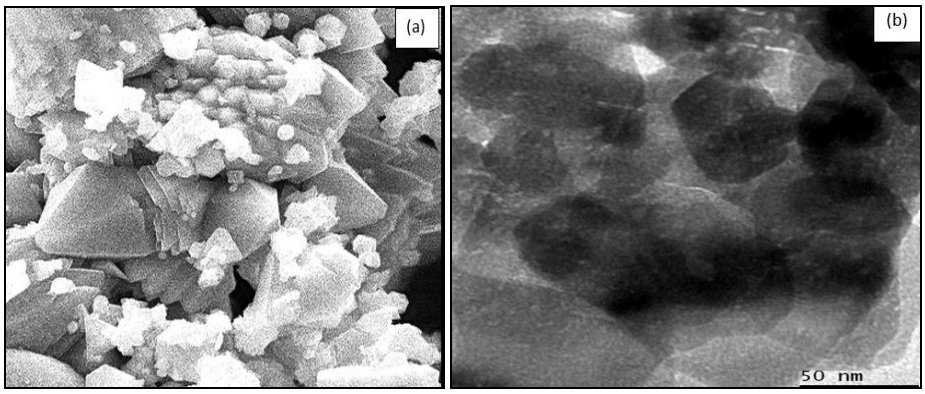

Fig 4: Morphological features of ZnO NPs from aqueous leaves extract of *Vitex altissima* (a) SEM micrographs and (b) TEM images

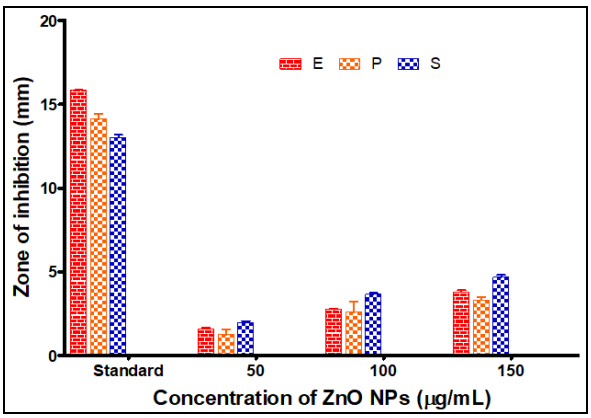

Fig 5: Antibacterial activity of ZnO NPs from aqueous leaves extract of *Vitex altissima* against pathogenic bacterial strains such as *E. coli*, *S. aureus* and *P. desmolyticum*

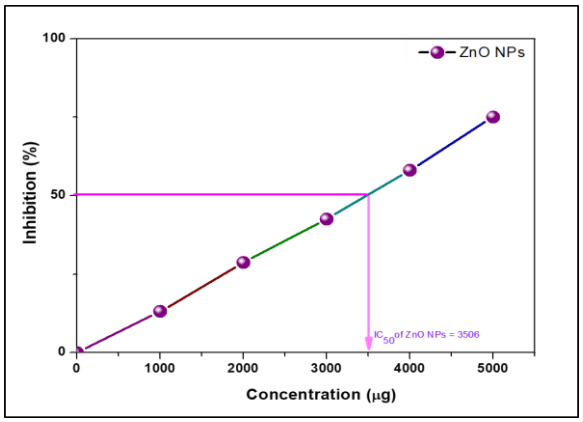

Fig 6: Antioxidant activity of ZnO NPs from aqueous leaves extract of *Vitex altissima* against DPPH radicals

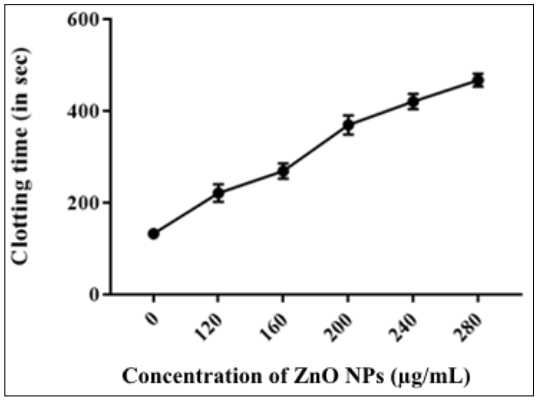

Fig 7: Plasma recalcification time of ZnO NPs using aqueous leaves extract of *Vitex altissima*

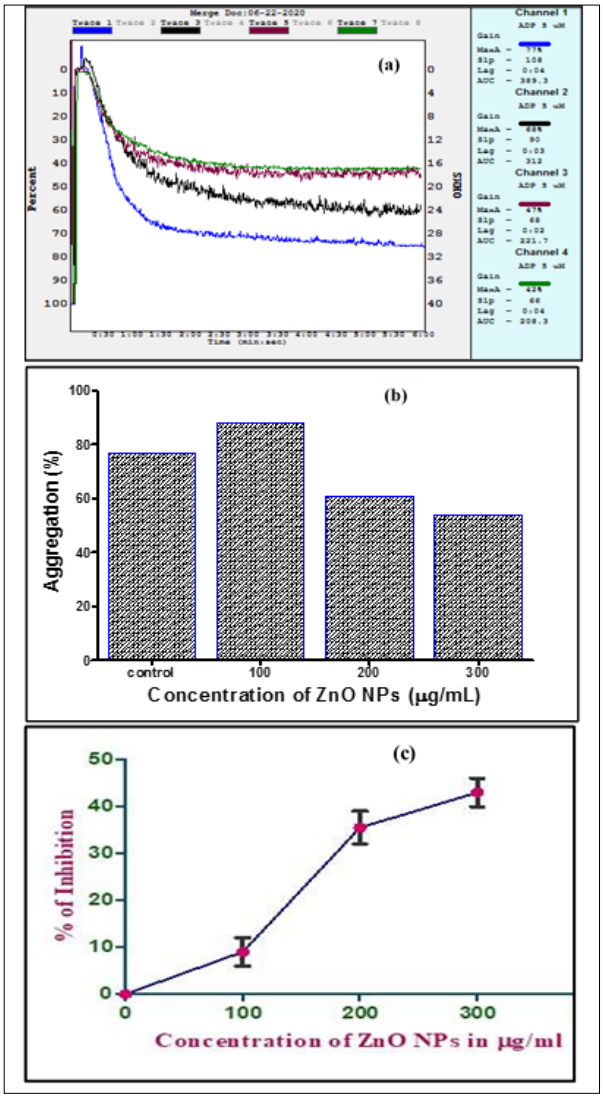

Fig 8: Platelet aggregation of ZnO NPs using aqueous leaves extract of *Vitex altissima* ADP as agonists (a) Traces of platelet aggregation: Trace 1 (ADP 10 µM); Trace 2 (ADP 10 µM+100 µg NPs); Trace 3 (ADP 10 µM+200µg of NPs); Trace 4 (ADP 10 µM+300 µg of NPs), (b) Dose dependent platelet aggregation % (c) Dose dependent platelet aggregation inhibition % of ZnO NPs

Table 1: Antibacterial activity of ZnO NPs from *Vitex altissima* against pathogenic bacterial strains

Samples	Treatment concentration	*S. Aureus* (S) Mean ± SE	*E.coli* (E) Mean ± SE	*P. desmolyticum* (P) Mean ± SE
Ciprofloxacin	5µg/ µL	13.03±0.16	15.83±0.03*	14.13±0.09
ZnO NPs	50µg/ µL	1.97±0.09	1..60±0.06	1.27±0.27
	100µg/ µL	3.67±0.09	2.77±0.09	2.60±0.06
	150µg/ µL	4.70±0.12	3.80±0.10	3.33±0.17

Values are the mean ± SE of inhibition zone in mm.

Conclusion

Zinc oxide nanoparticles (ZnO NPs) are synthesized by using *V. altissima* leaves extract by solution combustion method. The structural, optical, and morphological characteristics of ZnO NPs were characterized by PXRD, UV–Visible, FTIR, SEM, and TEM techniques. The PXRD pattern of ZnO NPs shows hexagonal wurtzite structure. The UV-Vis absorption study of ZnO NPs at 373nm indicates blue shifts compared to bulk ZnO NPs. The FTIR spectrum of ZnO NPs shows Zn-O vibrational stretching at 436 nm. The morphological feature of the ZnO NP is conical and hexagonal shape. ZnO NPs shows significant antibacterial activity against pathogenic bacterial strains. Also, the antioxidant activity of ZnO nanoparticles shows efficient activity by potentially scavenging DPPH radicals. Further, ZnO NPs exhibit anticoagulant activity and also act as an antiplatelet agent whereas it does not shows any hemolytic activity. These studies reveals that green synthesized ZnO NPs can be employed for future use in biomedical applications.

Acknowledgements

The authors are grateful to the UGC-RGNF, New Delhi, Government of India for financial assistance and also thanks for Tumkur University, proving the laboratories for research works are gratefully acknowledged.

References

1. Nair LS, Laurencin CT. Silver Nanoparticles: Synthesis and Therapeutic Applications. J. Biomed. Nanotechnol. 2007; 3(4): 301-316.
2. Elumalai K, Velmurugan S. Green synthesis, characterization and antimicrobial activities of zinc oxide nanoparticles from the leaf extract of *Azadirachta indica* (L). App.Sur. Sci, 2015; 345:329-336.
3. Boverhof DR, Bramante CM, Butala JH, Clancy SF, Lafranconi M, West J, *et al*. Comparative assessment of nanomaterial definitions and safety evaluation considerations. Regul Toxicol Pharmacol. 2015; 73(1):137-150.
4. Calestani D, Zha MZ, Mosca R, Zappettini A, Carotta MC, DiNatale V, *et al*. Growth of ZnO tetrapods for nanostructure-based gas sensors. Sensor and actuator B-chemical. 2010; 144:472-478.

5. Suresh C, Kelly JM, Ramesh R. Advances in the synthesis of ZnO nanomaterials for varistor devices. J. Materials Chem. 2013; 1:3268-3281.
6. Sasidharan NP, Chandran P, Sudheer Khan S. Interaction of colloidal zinc oxide nanoparticles with bovine serum albumin and its adsorption isotherms and kinetics, Colloids and Surf.B: Biointer. 2013; 102:195- 201.
7. Shaheer Akhtar M, Sadia Ameen, Shoeb Ansari A, O-Bong Yang. Synthesis and Characterization of ZnO Nano rods and Balls Nanomaterials for Dye Sensitized Solar Cells. J. Nano engineer. and Nanomanufact, 2011; 1:71-76.
8. Azizi S, Ahmad MB, Namvar F, Mohamad R. Green biosynthesis and characterization of zinc oxide nanoparticles using brown marine macroalga *Sargassum muticum* aqueous extract. Materials Letters. 2014; 116:275–277.
9. Liu B, Zeng HC. Hydrothermal synthesis of ZnO nanorods in the diameter regime of 50 nm. J. Am. Chem. Soc. 2003; 125:4430-4431.
10. Yan L, Wang GZ, Tang CJ, Wang HQ, Zhang L. Synthesis and photoluminescence of corn-like ZnO nanostructures under solvothermal-assisted heat treatment. Chem. Phys. Lett. 2005; 409:337-341.
11. Guo L, Ji Y, Xu H. Regularly shaped, single-crystalline ZnO nanorods with wurtzite structure. J. Am. Chem. Soc. 2002; 124:14864-14865.
12. Wang Z, Zhang H, Zhang L, Yuan J, Yan S, Wang C. Low-temperature synthesis of ZnO nanoparticles by solid-state pyrolytic reaction. Nanotechnol. 2003; 14:11-15.
13. Pillai SC, Kelly JM, McCormack DE, Brien PO, Ramesh RR. The effect of processing conditions on varistors prepared from nanocrystalline ZnO. J. Mater. Chem. 2003; 13:2586-2590.
14. Suresh D, Udayabhanu, Nethravathi PC, Lingaraju K, RajaNaika H, Sharma SC, *et al*. EGCG assisted green synthesis of ZnO nanopowders: Photodegradative, antimicrobial and antioxidant activities. Spectrochimica Acta Part A: Mol. Biomol. Spectro. 2015; 136:1467-1474.
15. Manjunath K, Ravishankar TN, Dhanith Kumar, Priyanka KP, Thomas Varghese, Raja Naika H, *et al*. Facile combustion synthesis of ZnO nanoparticles using *Cajanus cajan* (L.) and its multidisciplinary applications. Materials Res. Bull. 2014; 57:325-334.
16. Nie SM, Xing Y, Kim GJ, Simons JW. Nanotechnology applications in cancer. Annu.Rev. Biomed. Eng. 2007; 9:257.
17. Sridhar C, Subbaraju GV, Venkateshwarulu Y, Venugopal RT. New acylated iridoid glucosides from *Vitex altissima*. J Nat Prod. 2004; 67:2012-2016.
18. Manjunatha BK, Vidya SM, Krishna V, Mankani KM, Singh SD, Manohara YN. Comparative evaluation of wound healing potency of *Vitex trifolia* L. and *Vitex altissima* L. Phytother. Res. 2007; 21:457-461.
19. Raja Naika H, Krishna V. Antimicrobial activity of extracts from the leaves of *Clematis gouriana* ROXB. Inter. J. Biomed. Pharm.sci. 2006; 1:69-72.
20. Lingaraju K, Raja Naika H, Manjunath K, Nagaraju G, Suresh D, Nagabhushana H, *Rauvolfia serpentina*-Mediated Green Synthesis of CuO Nanoparticles and its Multidisciplinary Studies. Acta Metal. Sinica. 2015; 28(9):1134-1140.
21. Nagajyothi PC, Sreekanth TVM, Clemen O, Tettey, Jun YI, Heung Mook S. Characterization antibacterial, antioxidant, and cytotoxic activities of ZnO nanoparticles using *Coptidis Rhizoma*. Bioorganic Medicinal Chemistry Letters. 2014; 24(17):4298-4303.
22. Suresh D, Shobharani RM, Nethravathi PC, Kumar MAP, Nagabhushana H, Sharma SC. *Artocarpus gomezianus* aided green synthesis of ZnO nanoparticles: Luminescence, photo catalytic and antioxidant properties. Spectrochimica Acta Part A: Molecular and Bio molecular Spectroscopy. 2015; 141:128-134.
23. Quick AJ, Stanley-Brown M, Bancroft FW. A study of the coagulation defect in hemophilia and in jaundice. The American Journal of Medical Sciences. 1935; 190:501-511.
24. Born GV. Aggregation of blood platelets by adenosine diphosphate and its reversal. Nature. 1962; 194:27-29.
25. Dakshayani SS, Marulasiddeshwara MB, Sharath Kumar MN, Ramesh G, Raghavendra Kumar P, Devaraja S, *et al*. Antimicrobial, anticoagulant and anti-platelet activities of green synthesized silver nanoparticles using *Selaginella* (Sanjeevini) plant extract. International Journal of Biological Macromolecules. 2019; 131:787-797.
26. Nagabhushana H, Sunitha DV, Sharma SC, Prasad BD, Nagabhushana BM, Chakradhar RPS. Enhanced luminescence by monovalent alkali metal ions in Sr_2SiO_4: Eu^{3+} nanophosphor prepared by low temperature solution combustion method. J. Alloys and Comp. 2014; 575:192-199.
27. Lingaraju K, Raja Naika H, Manjunath K, Basavaraj RB, Nagabhushana H, Nagaraju G, *et al*. Biogenic synthesis of zinc oxide nanoparticles using *Ruta graveolens* (L.) and their antibacterial and antioxidant activities. App.Nano Sci. 2016; 6:703-710.
28. Sadia Ameen, Shaheer Akhtar M, Hyung Shik Shin. Semiconducting Nanostructures and Nano composites for the Recognition of Toxic Chemicals. Ori. J.chem. 2013; 29(3):837-860.
29. Wang J, Gao L. Wet chemical synthesis of ultra long and straight single-crystalline ZnO nanowires and their excellent UV emission properties. J. Mater. Chem. 2003; 13(10):2551-2554.
30. Zhang L, Jiang Y, Ding D, Povey M, York D. Investigation into the antibacterial behaviour of suspensions of ZnO nanoparticles (ZnO Nano fluids). J.Nano particle Res. 2007; 9(3):479-489.
31. Ramesh M, Anbuvannan M, Viruthagiri G. Green synthesis of ZnO nanoparticles using *Solanum nigrum* leaf extract and their antibacterial activity. Spectrochimica Acta Part A: Molecular and Biomolecular Spectroscopy. 2015; 136:864-870.
32. Suresh D, Nethravathi PC, Rajanaika H, Nagabhushana H, Sharma SC. Green synthesis of multifunctional zinc oxide (ZnO) nanoparticles using *Cassia fistula* plant extract and their photo degradative, antioxidant and antibacterial activities. Material Science Semiconducting Process. 2015; 31:446-454.
33. Lingaraju K, Raja Naika H, Nagabhushana H, Nagaraju G, *Euphorbia heterophylla* (L.) mediated fabrication of ZnO NPs: Characterization and evaluation of antibacterial and anticancer properties. Biocatalysis and Agricultural Biotechnology. 2019; 8:100-894.
34. Lingaraju K, RajaNaika H, Manjunath K, Basavaraj RB, Nagabhushana H, Nagaraju G, *et al*. Biogenic synthesis of zinc oxide nanoparticles using *Ruta graveolens* (L.) and their antibacterial and antioxidant activities. Applied Nanoscience. 2015; 1:1-8.
35. Stenberg PE, McEver RP, Shuman MA, Jacques YV, Bainton DF. A platelet alpha-granule membrane protein (GMP-140) is expressed on the plasma membrane after activation. Journal of Cell Biology. 1985; 101:880-886.
36. Drake TA, Morrissey JH, Edgington TS. Selective cellular expression of tissue factor in human tissues, implications for disorders of hemostasis and thrombosis. American Journal of Pathology. 1989; 134(5):1087-97.
37. Nandish MSK, Kengaiah J, Ramachandraiah C, Shivaiah A, Chandramma, Girish KS, *et al*. Anticoagulant, antiplatelet and fibrin clot hydrolyzing activities of flax seed buffer extract. Pharmacognosy Magazine, 2018; 14(S1): 175-183.
38. Tania L, Francesca S, Valentina C. Nanoparticles for hematologic diseases detection and treatment. Hematology and Medical Oncology. 2019; 4:1-12.
39. Lateef A, Ojo SA, Elegbede JA, Azeez MA, Yekeen TA, Akinboro A. Evaluation of some biosynthesized silver nanoparticles for biomedical applications: hydrogen peroxide scavenging, anticoagulant and thrombolytic activities. Journal of Cluster Science. 2017; 28(3):1379-1392.